Next Generation Wind Tunnels for Simulation of Straight-Line, Thunderstorm- and Tornado-Like Winds

by

Partha P. Sarkar[1] & Fred L. Haan, Jr.[1]

ABSTRACT

Researchers at Iowa State University (ISU) are developing next generation wind tunnels for studying primarily wind effects on structures. The Wind Simulation and Testing Laboratory in the Department of Aerospace Engineering and Engineering Mechanics will house facilities that simulate straight-line, thunderstorm- and tornado-like winds. This paper describes the motivation for advancing the state of the art of wind-structure interaction problems and the work currently underway at ISU.

A closed-circuit wind tunnel at ISU is currently being designed to accommodate two test sections (2.44 m x 1.83 m and 2.44 m x 2.29 m) with maximum wind speed capabilities of 50 m/s for aerodynamic testing and 40 m/s for testing in boundary-layer wind. It will have a gust generator that is capable of producing gusts up to 125% of the mean speed and an active lateral-turbulence generator that is capable of replicating the turbulence in hurricane winds. In addition, a microburst simulator and a tornado simulator are being designed. While the microburst simulator can produce a stationary/translating downdraft of 1.60 m in diameter and 25 m/s wind speed, the tornado simulator will produce a stationary or translating tornado-like vortex of up to 1.22 m in diameter with a swirl ratio of up to 2.0.

KEYWORDS: atmospheric boundary layer; next generation wind tunnel; thunderstorm simulation; tornado simulation; wind loads.

1.0 INTRODUCTION

Building wind tunnels with advanced capabilities will aid research efforts to understand the complex fluid structure interaction problems encountered in wind engineering design. Computer simulations currently are inadequate for design calculations because of the complexity of the fluid dynamics problems involved. Wind tunnels remain an integral component of the design process for wind sensitive structures.

Whether dealing with the aerodynamics of buildings, bridges or towers many issues remain to be fully resolved—including the role of non-stationary gust interactions, Reynolds number effects, and the significance of small-scale turbulence. Research into these issues is currently limited by the capabilities of existing wind tunnels. Building the next generation of such wind tunnels will contribute to the research infrastructure necessary to meet the challenges of wind hazards in this country. Better simulations of atmospheric flows will enhance our understanding of the various fluid structure interaction phenomena involved and greatly enhance our ability to develop mitigation measures.

[1] Wind Simulation and Testing Laboratory, Department of Aerospace Engineering and Engineering Mechanics, Iowa State University, 2271 Howe Hall, Room 1200, Ames, IA 50011-2271 USA

Understanding how the construction of wind tunnels with advanced capabilities constitutes a worthy endeavor requires some background into the use of wind tunnels in wind engineering and into the technical problems faced by wind engineers. This section provides such background by providing a general introduction to atmospheric boundary layer (ABL) wind tunnels—the wind engineer's tool of choice for the past several decades. Following this introduction, three distinct types of wind tunnels—for straight-line, thunderstorm-like and tornado-like winds—will be described.

2.0 BACKGROUND

2.1 Boundary-Layer Wind Tunnel

Wind tunnel simulation of the earth's atmospheric boundary layer is a well-established practice. Numerous researchers have contributed to the set of tools now in use for generating wind tunnel boundary layers that are several feet deep (for example, Cermak, 1971; Davenport, 1966; Cook, 1973; Farell and Iyengar, 1999). Conventional approaches employ a combination of passive devices such as spires, barrier walls, and floor roughness to generate boundary layers of the same scale as the geometric scaling of structural models placed in them.

It is assumed that atmospheric velocity variations can be adequately modeled by stationary mean and turbulent flow properties. This assumption means that despite the fact that hurricanes and gust fronts can have non-stationary characteristics, wind sensitive structures are tested in stationary flow environments. Wind tunnel turbulence intensities are matched to site values, and wind tunnel integral scales are scaled with the geometric scale of the structural models. While this conventional approach has served (and still serves) research and industrial needs for some time, the following two sections summarize how new tunnel capabilities can answer questions that cannot be addressed with the current generation of wind tunnels.

2.1.1 Turbulence Effects

The role of turbulence in the relevant fluid-structure interaction problems will influence the wind tunnel design. While some of the characteristics of atmospheric turbulence have been simulated sufficiently well for some time (for example, boundary layer velocity profiles, scaling of turbulence integral scales with model dimensions, etc.) other turbulence characteristics cannot be simulated precisely at all or cannot be simulated without considerable effort. This section briefly describes the role that turbulence plays in wind engineering and how new capabilities in wind tunnels can improve our understanding of these complex fluid-structure interaction problems.

Civil engineering structures do not, in general, have aerodynamic performance as their primary design goal. As a result, most civil engineering structures can be classified as bluff rather than streamlined bodies. Bluff bodies experience flow separation over significant portions of their surface. Bluff body aerodynamics differs from aerodynamics of streamlined bodies in that flow separation and reattachment play primary roles in pressure distributions about bodies of interest.

Free stream turbulence can modify the behavior of shear layers separating from bluff bodies. These modifications lead to flow structure changes and pressure distribution changes.

The role of turbulence in the aerodynamics of bluff bodies has been extensively documented in the literature (e.g., Gartshore, 1973; Kareem & Cermak, 1979; Hillier & Cherry, 1981; Bearman & Morel, 1983; Nakamura & Ohya, 1984; Kiya & Sasaki, 1985; Saathoff & Melbourne, 1997; and others). What is clear is that turbulence scales influence aerodynamic properties (such as rms and peak pressure coefficients). What is not clear is the extent of these influences or the precise mechanism of these influences.

When considering the smallest scales of turbulent velocity fluctuations, the inertial subrange is a relevant concept. The "inertial subrange" of a turbulent flow refers to that range of turbulent eddy scales between the large inviscid energy-containing scales and the small viscous diffusion scales. The size of the small, energy dissipating scales decreases with increasing Reynolds number—which accompanies an increase in the size of the inertial subrange. The size of the inertial subrange is relevant to bluff body aerodynamics because the size of the subrange impacts the amount of turbulent energy residing at small scales. Small scale content—particularly scales on the order of the thickness of the separated shear layer—has been shown by a number of researchers to have a significant effect on separated shear layer flow structure (Gartshore, 1973; Tieleman & Akins, 1990).

A significant difference in small-scale turbulence content can exist between wind tunnel and full-scale flows because wind tunnel Reynolds numbers can be as much as three orders of magnitude lower than those of atmospheric flows. To quantify small-scale content, a "small-scale spectral density parameter" was originally suggested by Melbourne (1979) and subsequently used by Tieleman and Akins (1990). This parameter is essentially a *scale-specific* turbulence intensity. Tieleman and Akins reported that wind tunnel simulations with insufficient small scale content resulted in poorer comparisons of pressure coefficients between model and full-scale results.

The above may not fully address all issues relating to Reynolds number mismatches. Rather, it illustrates one of the ramifications of failing to match Reynolds numbers in wind tunnel simulations. Decreasing Reynolds number disparities between model and prototype flows will increase our confidence in test results. Understanding the physics of *how* flows depend on Reynolds number will decrease the uncertainty associated with imperfect turbulence simulation. Wind tunnels capable of higher Reynolds numbers would enable study of such questions.

2.1.2 Non-Stationary Flow Simulation

In addition to Reynolds number and small-scale turbulence issues, large-scale turbulent gusts also constitute an important aspect of wind tunnel simulation. Passive turbulence generation techniques (such as the obstacles described previously) have been shown to produce only a limited range of possible integral scales (Bienkiewicz et al., 1983). These scales are often not large enough to match prototype scales. As a result, active turbulence generation schemes have been developed to produce integral scales up to an order of magnitude larger than those of passive techniques. These techniques generally involve grids, flaps, airfoils (and combinations of them) that are forced to oscillate (Bienkiewicz et al., 1983; Kobayashi et al., 1994; Cermak et al., 1995).

While such devices are useful for generating stationary velocity fluctuations, they have not generally been used to simulate the non-stationary gusts that can occur in hurricanes. Anemometry data from hurricanes has shown that velocity records are non-stationary at times (Schroeder & Smith, 1999). Thus far, however, no wind tunnel studies have investigated the impact of such non-stationarity on aerodynamic pressures on structures. The next generation of ABL wind tunnel should have the capability to conduct such tests.

In addition to simulating large-scale gusts, wind direction changes can be simulated with active turbulence generation equipment. Wind direction changes have been observed to significantly affect pressure distributions on building models in wind tunnels (Wu et al., 2001a; Wu et al., 2001b). Next generation ABL wind tunnels will also be used for furthering research of this type.

2.2 Thunderstorm Winds

Microbursts occur in thunderstorms where the weight of the precipitation and the cooling due to microphysical processes acts to accelerate the air downwards. They are characterized by a strong localized down-flow and an outburst of strong winds near the surface. Strong outflow winds develop as the downdraft air is forced to spread horizontally near the ground level.

Fujita (1985) termed microburst as a small downdraft having an outburst of damaging winds with the horizontal extent of the damaging winds being less than 4 km. This definition has been modified by radar meteorologists: they require the peak-to-peak differential Doppler Velocity across the divergent center to be greater than 10 m/s and the distance between these peaks be less than 4 km.

Thunderstorm winds have significant vertical velocity components and mean horizontal velocity distributions different from usual boundary-layer winds. It is also believed that the gust structure in a downdraft is much better correlated over its width than in more traditional boundary-layer flow, and hence will lead to larger overall loading of long structures. Thunderstorms are responsible for about 1/3 of the extreme gust speeds in the United States (Thom, 1969). In recent studies of extreme wind speeds in the United States, Vickery and Twisdale (1995) found that, outside of hurricane regions, up to 75% of the peak gust wind speeds occurred during thunderstorms. Selvam and Holmes (1992) undertook numerical modeling of the thunderstorm downdraft phenomenon, and were able to demonstrate reasonable agreement between a numerical model and limited full-scale data. Later, Holmes (1999) and Letchford and Illidge (1999) undertook physical model studies of a jet impinging on a wall and again found reasonable agreement between the numerical model, physical model and full-scale observations of a jet outflow velocity profile.

2.3 Tornado Winds

Tornadoes are vortices with significant tangential and vertical velocity components. Therefore, the flow field in a tornado is much different from the straight-line boundary-layer wind. Each year people die and civil infrastructure sustains damage due to tornados. According to Wind Hazard Reduction Coalition statistics (for more information, see www.windhazards.org), each year an average of 800-1000 tornados occur in the U.S. and cause 80 deaths (on average), 1500 injuries, and $850 million worth of damage. Although mostly associated with the region in the central states often referred to as “tornado alley,” tornados have occurred in all fifty states and also occur in coastal regions as hurricanes make landfall.

In spite of causing significant losses, tornados have received little attention from wind engineers. Statistics show that 90% of all recorded tornados are rated F2 or less (Bluestein, 1993) on the Fujita Scale—that is, they involve wind speeds less than 157 mph. It may be economically feasible to design structures to resist F2 tornados. For cases where structures cannot be designed to survive, shelters below or above ground can be designed to protect people from tornados. It can be argued that certain essential facilities such as power plants, hospitals, and airports should be designed for tornados of F3 intensity or higher. Any such design work, however, requires accurate information about the nature of the wind loads on structures due to tornados.

Determining tornado-induced wind loads is difficult for two reasons—because quantifying wind velocity magnitudes in tornados is difficult and because simulating tornados in a laboratory while measuring wind pressures on structures is non-trivial and has not been attempted systematically. Laboratory simulation of tornados to obtain wind loads on structures is considered later. With the latest instruments, equipment, and computing facilities, it is now possible to pursue these goals through fieldwork and through numerical and laboratory simulation.

2.3.1 Field Measurements

Beyond the use of storm damage, recent advances in field measurements have greatly enhanced current knowledge of tornados and the supercells that spawn them. For example, the VORTEX project (which stands for “Verification of the Origins of Rotation in Tornadoes Experiment”) (Rasmussen et al., 1994) was an effort to use advanced remote sensing equipment to conduct field measurements of tornados and tornadic storms.

One particular piece of field equipment that has proved to be useful is the “Doppler on Wheels” system (DOW). DOW systems measure wind velocities directly during a storm from single or multiple truck-based radars (e.g., Wurman, 1998, Wurman & Gill, 2000). In more recent years two DOW radars have been deployed in a pattern to allow dual-Doppler analysis. Whereas a single radar can measure the component of the wind along the line of site of the radar, a dual-Doppler analysis can determine the 3D characteristics of the flow field. The DOW radars have been upgraded to include a 2.33 m dish, with a 0.9 degree beam width. In a violent tornado in South Dakota, one of the radars was deployed within 1.7 km of the tornado, so that wind data were collected with resolution of 30 m x 30 m x 38 m (Wurman 1998). These wind observations from radar are both supporting existing theories, and in some cases, raising questions about the previous views of tornado behavior. For example, Doppler measurements are finding that the decay rate of the wind does not follow a Rankine curve, as is often assumed (Wurman & Gill 2000).

2.3.2 Numerical Simulation

Because of prior difficulties in collecting small-scale observations within and near a tornado, numerical simulations of tornadic flow have been performed as a tool to improve understanding of tornado dynamics, small-scale flow characteristics, and possible genesis mechanisms (e.g., Lewellen et al., 1997; Lewellen et al. 2000a). Many of the numerical models developed were patterned after existing laboratory simulators, and were based upon simplified forms of the governing equations.

In most of the prior studies conducting numerical simulation of tornados, the emphasis has been on processes influencing the general tornadic wind flow or on potential mechanisms for tornadogenesis or tornado dissipation. Such issues can be explored with grid spacings larger (roughly 50-100 m) than what is required to examine the fine-scale details of tornado wind structure near the ground. Because of the different focus of these earlier works, little information has been provided about wind variations near enough to the ground to impact most built structures. For instance, Lewellen (1993) states that the *maximum velocities will occur below the top of the ground boundary layer (roughly 100 m above surface)*—a result that has great significance for determining tornado-induced wind loads. Therefore, much more detail about the near-ground winds is needed.

2.3.3 Laboratory Simulation

Simulating tornados in laboratory environments is not a new concept. Many laboratory simulator designs have been based on the pioneering work of Ward (1972). The Ward simulator essentially consisted of a fan providing updraft at the top of a cylinder above a test area and guide vanes and rotating screens around the test area to provide angular momentum to converging flow. Subsequent efforts—based on the Ward model—at Purdue University (Church et al., 1979), the University of Oklahoma (Jischke & Light, 1983) and that of Davies-Jones (1976) employed various means to improve the similarity between laboratory simulations and full-scale tornado events.

These laboratory simulations were aimed at greater understanding of the tornado vortex itself. However, numerical simulation has overtaken physical simulation as the tool of choice for tornado studies—both because of cost and because of versatility. While both laboratory and numerical simulation efforts have revealed a great deal about tornado structure (Lewellen, 1993), physical simulation of tornados *for the purpose of studying the tornado* may no longer be useful. For the purpose of quantifying tornadic wind loads on structures, however, physical simulation is a necessity.

The fluid mechanical complexity of flow-structure interaction problems relevant to buildings and engineered structures require that physical modeling (usually wind tunnels) be a fundamental design tool. Computers, in most cases, do not have the capacity for the Reynolds numbers and geometric complexity involved. This is also true of flow-structure interactions problems involving tornados.

Chang (1971) and Jischke & Light (1983) both modified the basic Ward design and added a small building model with pressure taps. These efforts found mean surface pressures to be significantly higher (3-5 times) in swirling, tornado-like vortices than in straight-line boundary layer flows. This suggests that when estimating tornado-induced wind loads on structures, it is not sufficient to use a conventional wind tunnel running with tornado wind velocities.

3. CURRENT WORK

3.1 Boundary-Layer Wind Tunnel Facility

At this point, much of the rough design of the wind tunnel has been completed. Rough sizing and layout of various components including the test sections, turning sections, and fan has been completed (Figure 1). This design incorporates non-stationary flow capabilities and a high velocity capacity of 50 m/s (112 mph) along with a large cross section to accommodate realistic models. The wind tunnel will be of closed-circuit type with the option of running in an open-circuit mode. It will have two test sections, one for aerodynamic testing that is 2.44 m (8 ft) wide by 1.83 m (6 ft) high followed by a test section to simulate atmospheric boundary layer wind that is 2.44 m (8 ft) wide by 2.29 m (7.5 ft) high. The maximum speed in the ABL test section will be 40 m/s (89 mph). Increased velocity capability will allow larger Reynolds numbers—with the accompanying increase in small-scale turbulent spectral content. A large working cross section will accommodate both large-scale models and large-scale velocity structures.

The major component remaining to be designed is the gust front generator that will involve bypass venting for the wind tunnel. This bypass vent will connect a portion of the tunnel upstream of the test section with a portion downstream. Computer-controlled valves will be used to control how much air is vented through the test section thus modifying the velocity in the test section. Preliminary calculations show that variations in flow velocity of up to 25% of the mean wind speed can be obtained.

Other design details include final specifications for all parts including the fan, the motor, turning vanes, turbulence screens, honeycomb sections, etc. The selected fan is of 2.74 m (9ft) diameter with capability of 220 m^3/s (465,000 cfm) flow rate driven by a 260 kW (350 hp) AC motor. The open circuit mode will be achieved by removing the set of turning vanes at the two successive corners that follow the test sections. The turning vanes will be moved on rails to the duct that connects these corners and this duct will be isolated from rest of the wind tunnel to make the flow circuit U-shaped. It is also planned to use one set of turning vanes as a heat exchanger to minimize the pressure losses in the tunnel.

3.2 Microburst Simulation

The schematic diagram for a downdraft flow is shown in Figure 2, and the experimental setup for the microburst simulator is shown in Figure 3. A honeycomb and two screens were used to reduce the turbulence of the issuing jet. A 3:1 area contraction was used at the nozzle end to make the velocity of the issuing jet uniform. The diameter (D) of the jet nozzle was 203 mm (8”). The distance (H) of the ground plane or impinging platform from the jet nozzle could be varied from a minimum of 203 mm (8”) to a maximum of 826 mm (32.5”). For the current work, H/D = 2.89 and H/D = 4.06 were used. Henceforth, these two heights are termed as H23 and H32, respectively. The H/D ratio for this study was chosen to be around the median H/D value of a microburst that varies in between 0.75 to 7.5. Two jet velocities were used, V_0 = 9.57 m/s (31.4 ft/s) and V_0 = 16.17 m/s (52.0 ft/s). Henceforth, these two velocities are termed as V31 and V52, respectively. The velocity profiles were measured at distances of 2D and 3D from the center of the jet and the pressures on the buildings were also measured at those two locations as well as directly under the jet (i.e., at 0D). The building model used was a 25.4 mm (1”) cube with 21 pressure taps uniformly spaced along its centerline; 7 taps on each of the front, roof and rear of the building. Pressures on the ground plane along the centerline of the jet were measured using 22 taps.

Velocity measurements were done using a DANTEC MiniCTA with a single hot wire. Flow visualization was achieved using a smoke generator, and pressure measurements were conducted using seven Validyne DP-45 transducers with each having a maximum capacity of ±0.89 inH_2O.

Smoke flow visualization is shown in Figure 4 for a stationary jet. The horizontal velocity profiles at 2D (distance from the center of the jet) are plotted for two different heights of the jet as shown Figure 6. The profiles are compared with the empirical profile of Rajaratnam (1976), (Blevins, 1984), given by

$$\frac{U}{U_m} = e^{-0.693[(z-\delta)/b]^2}, \quad z \geq \delta, \qquad \text{Eqn. 1}$$

where δ is the height z from the ground plane at which the horizontal velocity U is maximum (U_m), and b is the height z where velocity is $U_m/2$ (Figure 5). Also plotted is Wood's (1999) empirical profile given by

$$\frac{U}{U_m} = 1.55\left(\frac{z}{b}\right)^{1/6}\left[1-\mathrm{erf}\left(0.7\frac{z}{b}\right)\right], \qquad \text{Eqn. 2}$$

where the variables U, U_m, z and b have been defined earlier and erf( ) is the error function. There is close agreement between the experimental and the empirical profiles. They are also compared with the experimental profile of Letchford & Illidge (1999).

3.3 Tornado Simulation

Small-scale models of the tornado simulator were built as design tools for the prototype. These were built to test concepts that advance the state of the art of laboratory tornado simulators beyond that based on the Ward simulator (Ward, 1972).

The first of the two simulators consists of a circular duct (diameter of 356 mm, 14 in.) that is vertically fixed to a trolley (Figure 7). It is covered at the top. A motor (0.75 kW or 1 hp, maximum 1750 rpm) drives a 5-blade vane located inside the duct through a pulley and shaft arrangement. The duct has a clearance of 127 mm (5 in.) from the top followed by a 102 mm (4 in.)–thick honeycomb plus screens. The 5-blade vane is 152 mm (6 in.) in length and is located below the honeycomb. There is a 356 mm (14 in.) gap between the vane and the exit of the duct. There is a deflector mounted at the duct exit to separate the updraft from the downdraft that occurs near the periphery of the duct. A variable speed motor drives the trolley so that the effect of translation speed on the tornado-like vortex can be studied. The distance between the ground plane and the bottom of the duct can be varied up to 584 mm (23 in.). There are two ground planes that can be separately used in this experimental setup. The first one has a circular opening covered by a slotted plate for injecting smoke or mist from underneath the ground plane to help visualize the flow. Two mist generators were used to produce mist for visualizing the vortex (Figure 8). The second ground plane has several pressure ports connected to a dedicated set of Validyne transducers to measure pressures on the ground surface underneath the vortex. The surface ground pressures were measured underneath the vortex (Figure 9) and compared with those obtained using Rankine vortex theory. They are comparable, but some differences exist. This is expected because the tornado vortex is somewhat different from a Rankine vortex in the free vortex region near the ground plane.

For the purpose of exploring different design configurations of the tornado simulator, a water-based simulator was also constructed (Figure 10). Water is often a better visualization medium than air. The water tank used here is a hexagonal glass tank. The height of the tank is 0.76 m (30 in.). The across panel dimension is 0.56 m (22 in.). The basic design of this simulator is the same as the tornado simulator mentioned earlier with minor differences. Due to the small size of this simulator, creating additional components are relatively inexpensive compared to the air-based tornado simulator. New blade assemblies and ducts can be interchanged with ease. This will aid the design process in terms of determining the best blade and duct assembly configuration for producing accurate representations of tornado vortices.

Visualization is accomplished by introducing glitter into the water and by using Particle Image Velocimetry (PIV) whose setup is shown in Figure 10. The velocity vectors were obtained on horizontal and vertical planes. The tangential velocity vectors at Z = 25 mm from the ground plane for the case where a screen (102 mm in diameter and 102 mm in height) was used without any surrounding duct at a height of 204 mm from the ground plane are shown in Figure 11.

Table 1 shows several parameters by which similarity between atmospheric and laboratory tornado vortices can be quantified. Aspect ratio is defined as the height of the vortex divided by the radius of the vortex core. Swirl ratio is the ratio of the vortex circulation compared to the accompanying flow rate into it. Radial Reynolds number is calculated using the radial velocity component of the tornado vortex flow. The parameters in this table for the ISU prototype simulator have been estimated based on the design and should be considered target parameters. The diameter of the simulated vortex near the ground for the prototype simulator is expected to be about 1.22 m (4 ft.) for a swirl ratio of 1.0 when the ground plane is 1.83 m (6 ft) from the ground. The diameter of the vortex will increase with reduced distance of the ground plane from the bottom of the rotating mechanism. This will allow structural model scales from 1:100, required for low-rise buildings, to 1:500, required for high-rise buildings and large structures. The surface friction on the ground plane will be scaled as per the geometric scale used for each model. The prototype simulator can translate for a distance of 3.05 m (10 ft) at a constant speed of 4.5 m/s (10 mph). The test section will be 6.1 m (20 ft) wide by 1.83 m (6 ft) high and 9.1 m (30 ft) length.

4.0 SUMMARY

This paper presents the need for the next generation wind tunnels for simulation of straight-line, thunderstorm and tornado-like winds and describes the current effort that is underway at Iowa State University.

5.0 REFERENCES

Bearman, P.W., Morel, T., "Effect of Free Stream Turbulence on the Flow Around Bluff Bodies," *Prog. Aerospace Sci.*, v. 20 (1983) 97-123.

Bienkiewicz, B., Cermak, J.E., Peterka, J.A., Scanlan, R.H., "Active Modeling of Large-Scale Turbulence." *Journal of Wind Engineering and Industrial Aerodynamics*, v. 13 (1983) 465-475.

Blevins, R. D, *Applied Fluid Dynamics Handbook*, Van Nostrand Reinhold Co, New York (1984).

Bluestein, H. B., "A Review of Tornado Observations," *The Tornado: Its Structure, Dynamics, Prediction, and Hazards*, ed. Church, Burgess, Doswell, Davies-Jones, American Geo. Mon. 79 (1993).

Cermak, J.E., "Laboratory simulation of the atmospheric boundary layer," *AIAA Journal*, 9, 9, (1971).

Cermak, J.E., Leighton, S.C., Leffler, R.D., "Wind-tunnel modeling of the atmospheric surface layer." *Journal of Wind Engineering and Industrial Aerodynamics*, v. 54/55 (1995) 505-513.

Church, C.R., J.T. Snow, G.L. Baker, E.M. Agee, "Characteristics of tornado-like vortices as a function of swirl ratio: A laboratory investigation," *Journal of the Atmospheric Sciences*, v. 36, (1979) 1755-1776.

Chang, C.C., "Tornado Effects on Buildings and Structures with Laboratory Simulation," *Proc. Third International Conference on Wind Effects on Buildings and Structures*, Tokyo, Japan, (1971) 231-240.

Cook, N.J., "On Simulating the Lower Third of the Urban Adiabatic Boundary Layer in a Wind Tunnel." *Atmospheric Environment*, v. 7 (1973) 691-705.

Davenport, A.G., "The treatment of wind loading on tall buildings," Proc. Symp. On Tall Buildings, (1966).

Davies-Jones, R.P., "Laboratory Simulation of Tornadoes," *Proceedings of the Symposium on Tornadoes, Assessment of Knowledge and Implications for Man*, ed. R.E. Peterson, Texas Tech University, (1976) 151-174.

Farell, C., Iyengar, A.K.S., "Experiments on the wind tunnel simulation of atmospheric boundary layers," *Journal of Wind Engineering and Industrial Aerodynamics*, v. 79 (1999) 11-35.

Fujita, T. T. *The Downburst: Microburst and Macroburst*, The University of Chicago Press, (1985).

Gartshore, I.S. *The effects of free stream turbulence on the drag of rectangular two-dimensional prisms*. Boundary Layer Wind Tunnel Laboratory 4-73, University of Western Ontario, (1973).

Hillier, R., Cherry, R.J., "The effect of stream turbulence on separation bubbles." *Journal of Wind Engineering and Industrial Aerodynamics*, v. 8 (1981) 49-58.

Holmes, J.D., "Modelling of extreme thunderstorm winds for wind loading of structures and risk assessment," 10th Int. Conf. on Wing Engineering, Copenhagen, 21-24 June, (1999).

Jischke, M. C., Light, B. D., "Laboratory Simulation of Tornadic Wind Loads on a Rectangular Model Structure," Proc. Sixth International Conference on Wind Engineering, v. 1, Australia & New Zealand (1983).

Kiya, M., Sasaki, K., "Structure of large-scale vortices and unsteady reverse flow in the reattaching zone of turbulent separation bubble." *Journal of Fluid Mechanics*, v. 154 (1985) 463-491.

Kareem, A., Cermak, J.E., "Wind-tunnel simulation of wind structure interactions." *ISA Transactions*, v. 18, n. 4 (1979) 23-41.

Kobayashi, H., Hatanaka, A., Ueda, T., "Active simulation of time histories of strong wind gust in a wind tunnel." *Journal of Wind Engineering and Industrial Aerodynamics* v. 53 (1994) 315-330.

Letchford, C.W. and Illidge, G. "Turbulence and topographic effects in simulated thunderstorm downdrafts by wind tunnel jet", 10th Int. Conf. on Wing Engineering, Copenhagen, 21-24 June, (1999).

Lewellen, W. S., "Tornado Vortex Theory," in Church et al., eds., *The Tornado: Its Structure, Dynamics, Prediction, and Hazards*, Geophysical Monograph 79, American Geophysical Union, (1993) 19-39.

Lewellen, W. S., D. C. Lewellen, R. I. Sykes, "Large-eddy simulation of a tornado's interaction with the surface," *J. Atmos. Sci.*, v. 54, (1997) 581-605.

Lewellen, D. C., W. S. Lewellen, J. Xia, "The influence of a local swirl ratio on tornado intensification near the surface," *J. Atmos. Sci.*, v. 57, (2000a) 527-544.

Melbourne, W.H., "Turbulence Effects on Maximum Surface Pressure – A Mechanism and Possibility of Reduction." *Wind Engineering, Proc. of Fifth International Conference.* Pergamon Press, (1979).

Nakamura, Y., Ohya, Y., "The effects of turbulence on the mean flow past two-dimensional rectangular cylinders." *Journal of Fluid Mechanics*, v. 149 (1984) 255-273.

Rajaratnam, N., *Turbulent Jets*, Developments in Water Science, 5, Elsevier Scientific Publishing Company, Amsterdam (1976).

Rasmussen, E.N., Straka, J.M., Davies-Jones, R., Dowell III, C.A., Carr, F.H. Milts, M.D., MacGorman, D.R. "Verification of the origins of rotation in tornadoes experiment: VORTEX," *Bulletin of the American Meteorological Society*, v. 75, (1994) 995-1006.

Saathoff, P.J., Melbourne, W.H., "Effects of free-stream turbulence on surface pressure fluctuations in a separation bubble." *Journal of Fluid Mechanics*, v. 337 (1997) 1-24.

Selvam, R.P. and Holmes, J.D. Numerical simulation of thunderstorm downdrafts", JWEIA, 41-44, pp. 2817-2825, (1992).

Schroeder, J.L., Smith, D.A., "Hurricane Bonnie wind flow characteristics as determined from WEMITE." *Wind Engineering into the 21st Century*, *Proc. of Tenth International Conference on Wind Engineering*, (1999) 329-335.

Thom, H.C.S. New distributions of extreme wind speeds in the United States, J. Structures Div., ASCE, 94, 1787-1801, (1969)

Tieleman, H.W., Akins, R.E., "Effects of Incident Turbulence on Pressure Distributions on Rectangular Prisms." *Journal of Wind Engineering and Industrial Aerodynamics,* v. 36, (1990) 579-588.

Vickery, P. J. and Twisdale, L.A. Analysis of thunderstorm occurrences and wind speed statistics, JWEIA, 55, 813-821, (1995).

Ward, N.B. (1972) The Exploration of Certain Features of Tornado Dynamics using a Laboratory Model. *J. of the Atmospheric Sciences*, 29, 1194-1204.

Wood, G. S and Kwok, K. C. S. "Physical and Numerical Modeling of Thunderstorm Downbursts", Wind Engineering into the 21st Century, Proc. of the 10th Intl. Conf. on Wind Eng., eds. A. Larsen et al., Denmark, June (1999), pp. 1919–1924.

Wu, F., Sarkar, P.P., Mehta, K.C., "Full-scale study of conical vortices and roof corner pressures." *Wind & Structures*, v. 4, n. 2 (2001) 131-146.

Wu, F., Sarkar, P.P., Mehta, K.C., Zhao, Z. "Influence of incident wind turbulence on pressure fluctuations near flat-roof corners." *Journal of Wind Engineering and Industrial Aerodynamics,* v. 89, (2001) 403-420.

Wurman, J. "Preliminary results from the ROTATE-98 tornado study," *Preprints, 19th Conf. on Severe Local Storms*, Minneapolis, MN, 14-18 September, (1998) 120-123.

Wurman, J., Gill, S. "Finescale radar observations of the Dimmitt, Texas (2 June 1995), tornado," *Mon. Wea. Rev.*, v. 128, (2000) 2135-2164.

TABLE 1. LABORATORY TORNADO SIMULATOR PARAMETERS

	Swirl Ratio	Aspect Ratio	Radial Reynolds No.
Atmospheric Range	0.050-2.0	0.2-3.0	1e9-1e11
Dallas Tornado	0.8	3.0	2e9
Purdue Simulator	0.1-1.0	0.3-3.0	4.1e3-1.2e5
Oklahoma Simulator	0.0-0.8	1.2	-
ISU Simulator	0.1-2.0	0.5-3.0	up to 1e6

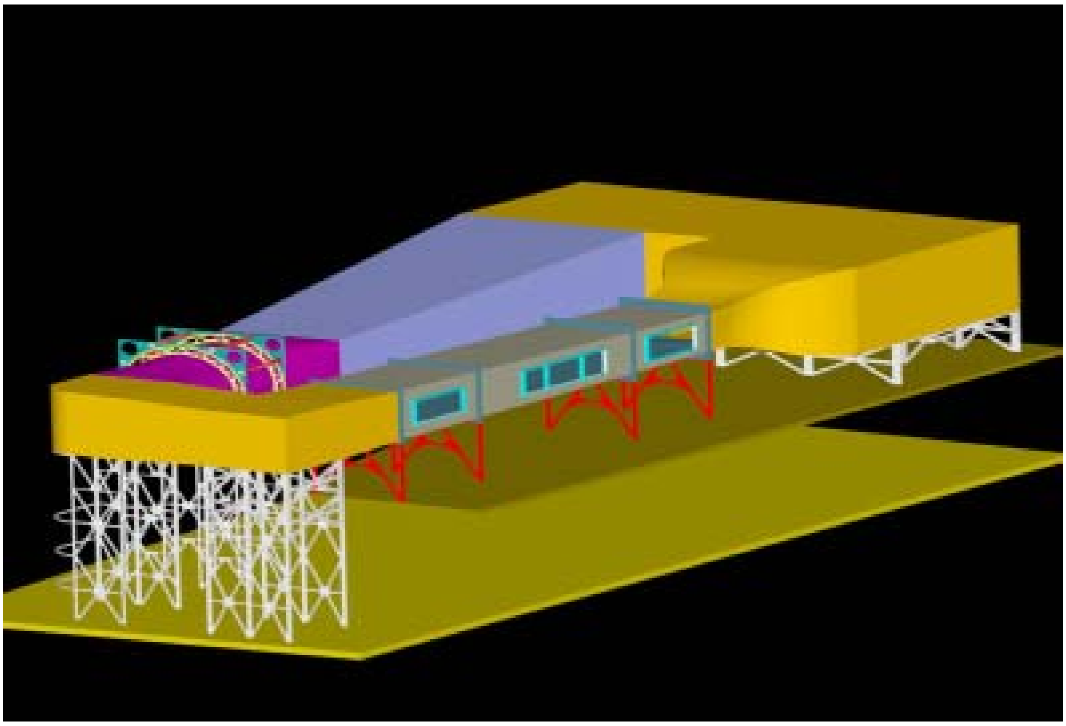

Figure 1 Three-dimensional rendering of the design for the atmospheric boundary layer wind tunnel.

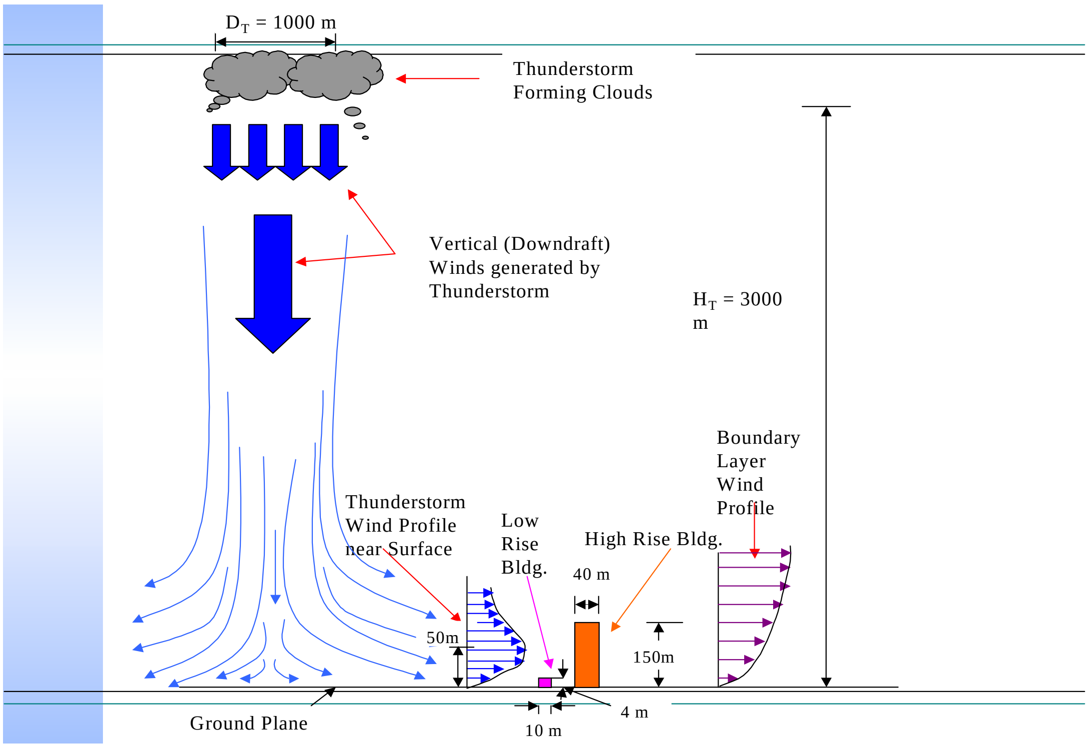

Figure 2. Schematic view of a typical downdraft flow showing the developed boundary-layer profile of horizontal flow field as compared to a straight-line boundary-layer wind profile

Figure 3. Experimental setup for the model microburst simulator

Figure 4. Microburst flow visualization with smoke

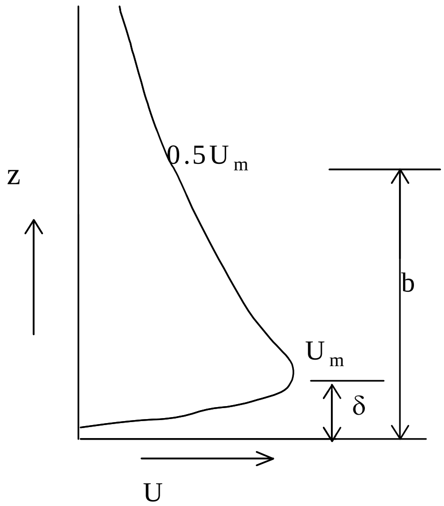

Figure 5. Boundary-layer horizontal velocity profile in an impinging jet

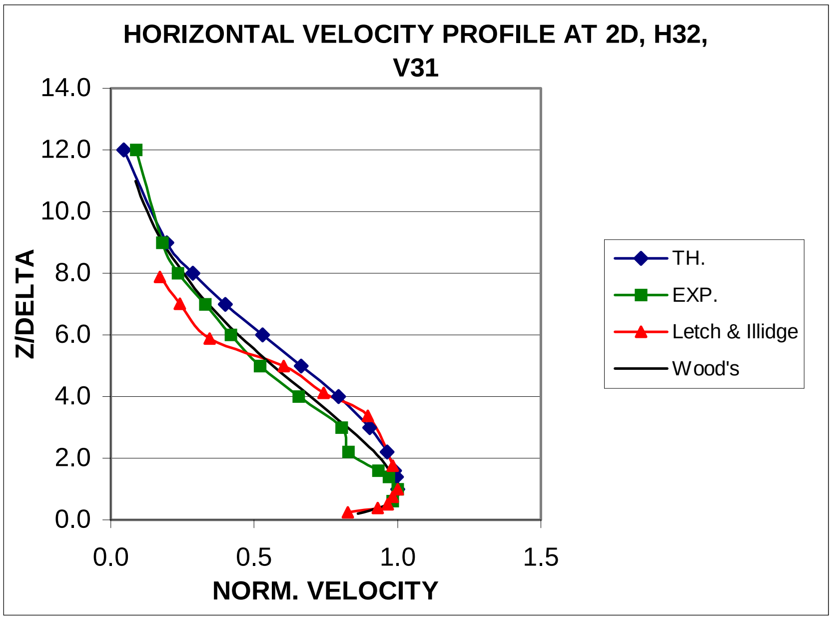

Figure 6. Comparison of normalized velocity profiles at 2D distance from the center of the microburst (D diameter). EXP. ISU experiment, TH. Blevin's (1984) Profile

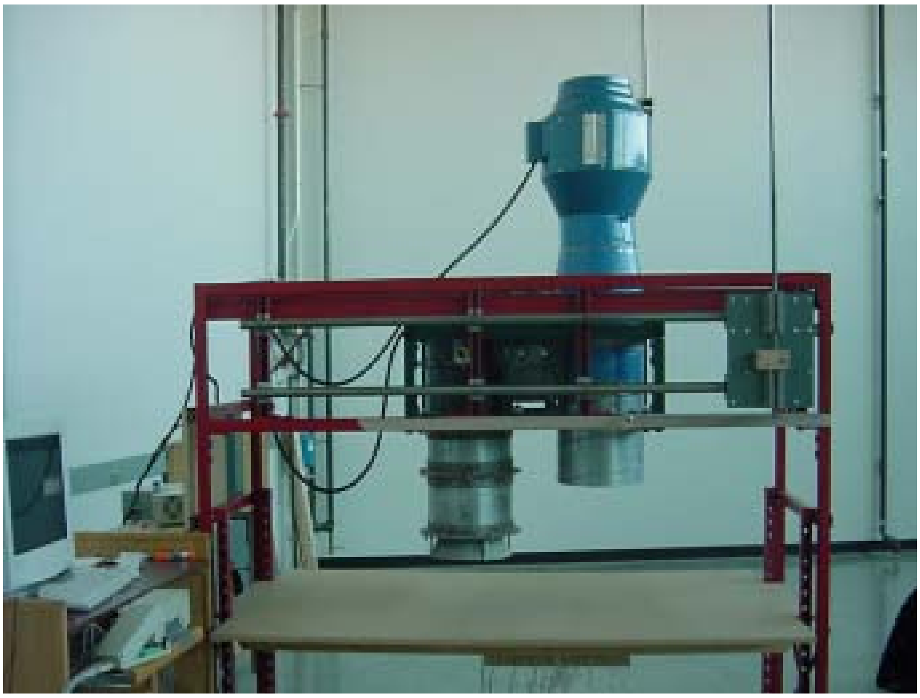

Figure 7. View of the model microburst/tornado simulator (1:5 scale) at ISU

Figure 8. Tornado flow visualization with mist (fine water particles in air)

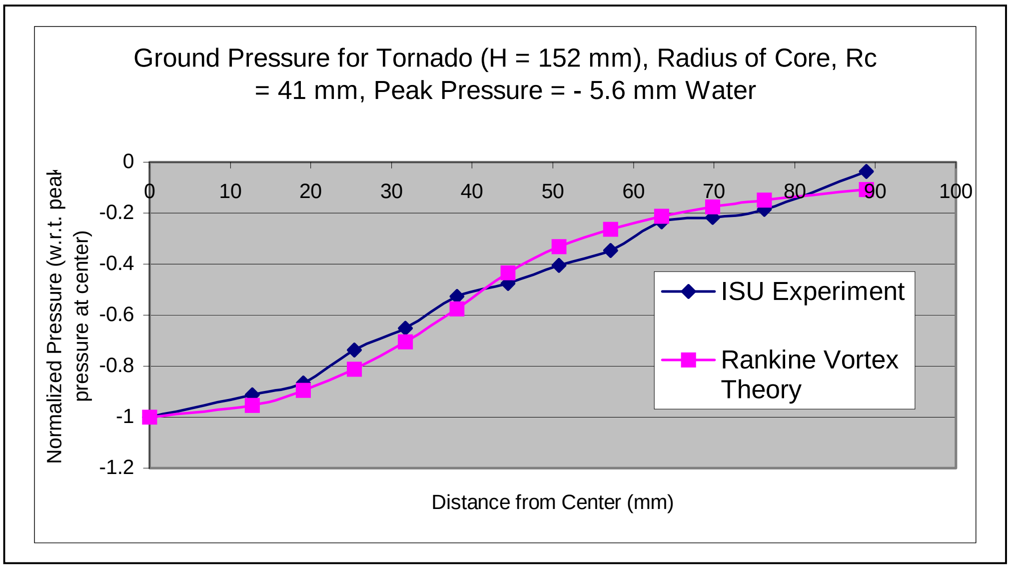

Figure 9. Normalized pressure distribution as measured underneath the tornado-like vortex on the ground plane compared with Rankine vortex

Figure 10. Experimetal setup for PIV measurement for flow visualization and measurement in water simulator

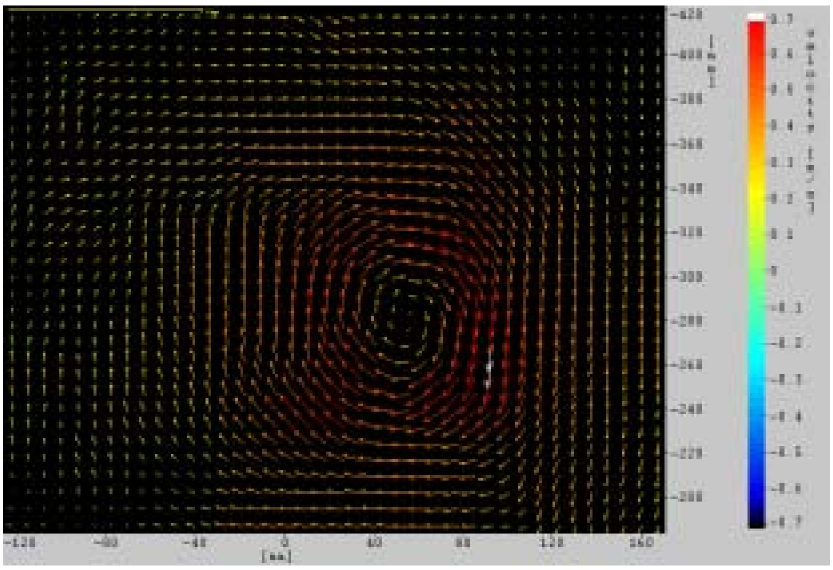

Figure 11. Tangential velocity vectors in the water simulator at z = 25 mm from ground plane. A screen (102 mm D and 102 mm H) without duct at 203 mm from ground plane was used to generate the vortex.